

Deep inelastic lepton-hadron scattering as a test of perturbative QCD

W.L. van Neerven ^a

^aInstituut-Lorentz, University of Leiden, P.O. Box 9506, 2300 RA Leiden, The Netherlands

Exploration of the small x kinematic region by the HERA experiments led to a revival of some models which existed before the advent of Quantum Chromo Dynamics (QCD) as the theory of the strong interactions. Predictions of these models for the deep inelastic structure functions are compared with those given by QCD. Future experiments will concentrate on the large x -region and we will discuss some issues which are important for the test of QCD. In particular we emphasize the next-to-next-to-leading (NNLO) order analysis of the structure functions and the determination of the strong coupling constant α_s . We also make some critical remarks about the relevance of so called large corrections in the small and large x -region.

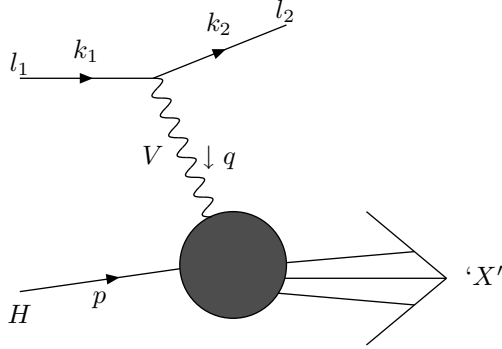


Figure 1. Kinematics of deep inelastic lepton-hadron scattering.

1. Introduction

Deep inelastic lepton-hadron scattering is given by the following process (see Fig. 1)

$$l_1(k_1) + H(p) \rightarrow l_2(k_2) + 'X'. \quad (1)$$

Here $'X'$ denotes any inclusive final hadronic state. The in and outgoing leptons are represented by l_1 and l_2 respectively and the hadron is denoted by H . On the Born level the reaction proceeds via the exchange of one of the vector bosons V of the standard model which are given by γ , Z and W^\pm . The kinematic variables needed

in this paper are defined by

$$q^2 = -Q^2 < 0, \quad \nu = \frac{p \cdot q}{M}, \quad x = \frac{Q^2}{2M\nu},$$

$$W^2 = (p + q)^2 = 2M\nu - Q^2 + M^2, \quad (2)$$

where W represents the CM energy of the virtual boson-hadron system. The most interesting quantities under study are the structure functions denoted by $F_i(x, Q^2)$ ($i = 2, 3, L$) which provides us with information about the strong interaction between the quarks and gluons. Besides these structure functions one can also study other observables for instance those which are related to the production of jets. However due to a lack of space we will limit ourselves to a discussion of the structure functions only.

2. QCD and alternative models

Immediately after the first experiments carried out at SLAC [1]¹ several models were proposed to explain the behaviour of the structure functions. The most prominent among them are

- a. Light Cone Expansions [3]
- b. Parton Model [4]
- c. Vector Meson Dominance (VMD) [5]
- d. Regge Pole Model [6]

¹Similar experiments were also carried out at DESY see [2]

e. Dual Resonance Models

One could also add the BFKL [7] approach which appeared later on the scene than the models above. It can be considered as a merger of ideas put forward by the models mentioned under b and d.

2.1. Light Cone Expansions

Suppressing Lorentz indices the structure function can be written as

$$F(x, Q^2) = \frac{1}{4\pi M} \int d^4 z e^{iq \cdot z} \langle p | [J(z), J(0)] | p \rangle, \quad (3)$$

In the commutator above $J(z)$ represents the electro-weak current. In the rest frame of the proton, with $p = (M, 0)$, the exponent becomes $q \cdot z \sim \nu(z_0 - z_3) - xMz_3$ for $\nu \gg M$. Using Fourier analysis the integral only gets contributions in the region $q \cdot z = \text{const.}$. Therefore the integrand is dominated by the space-time region [3]

$$|z_0 - z_3| < \frac{1}{\nu}, \quad z_0 < \frac{1}{xM}, \quad z_3 < \frac{1}{xM}. \quad (4)$$

Furthermore because of Einstein microcausality the commutator of the electro-weak currents vanishes for $z^2 < 0$. From the latter and Eq. (4) one infers that the integrand is dominated by the light cone region $z^2 < 1/Q^2$ provided Q^2 is chosen to be sufficiently large. Therefore this variable is the relevant scale for the Operator Product Expansion (OPE) and the Parton Model which are the ingredients of perturbative QCD. However there are other arguments in the literature [8] leading to the claim that the distance between absorption and emission of the virtual vector boson, given by $z_0 \sim z_3 = 1/xM$, is the relevant scale. If $1/xM > 2R$, where R denotes the radius of the hadron, the virtual vector boson fluctuates into a hadronic system which interacts with the hadron H in Fig. 1 so that one deals with hadron-hadron collisions rather than vector boson-hadron scattering. When x is sufficiently small the inequality above is satisfied ² and one enters the so called

² For the proton, where $R = 5 \text{ GeV}^{-1}$, this would mean that $x < 0.1$

Regge region where $2M\nu \gg Q^2$. Note that at this moment this inequality can be experimentally only realized when the vector boson is represented by the photon. The inequality $1/xM > 2R$ is the justification of small x physics which is at the basis of e.g. the Regge Pole Model and Vector Meson Dominance.

When the light cone region dominates one can make the Operator Product Expansion (OPE) [3]

$$[J(z), J(0)] \Big|_{z^2 \sim 0} = \sum_{\tau} \sum_N C^{N,\tau}(z^2 \mu^2) O^{N,\tau}(\mu^2, 0), \quad (5)$$

where τ and N denote the twist and spin of the operator $O^{N,\tau}$ respectively. Both the coefficient function $C^{N,\tau}$ and the operator $O^{N,\tau}$ are understood to be renormalized and μ denotes the renormalization scale which later on can be identified with the factorization scale. The operator product expansion has been proven for some quantum field theories in the context of perturbation theory. Assuming that it also holds in QCD one can express the N th moment of the structure function as follows

$$\int_0^1 dx x^{N-1} F(x, Q^2) = \sum_{\tau} \left(\frac{M^2}{Q^2} \right)^{\frac{\tau}{2}-1} A^{(N),\tau}(\mu^2) \mathcal{C}^{(N),\tau} \left(\frac{Q^2}{\mu^2} \right). \quad (6)$$

In momentum space the operator matrix element and the coefficient function are defined by

$$A^{(N),\tau}(\mu^2) = \langle p | O^{N,\tau}(\mu^2, 0) | p \rangle, \quad (7)$$

and

$$\mathcal{C}^{(N),\tau} \left(\frac{Q^2}{\mu^2} \right) = \int d^4 z e^{iq \cdot z} C^{N,\tau}(z^2 \mu^2), \quad (8)$$

respectively.

2.2. Parton Model

For leading twist, i.e. $\tau = 2$, the results of the operator product expansion are reproduced by the Parton Model. The Bjorken scaling variable x , defined in Eq. (2), has a nice interpretation if one describes lepton-proton scattering in

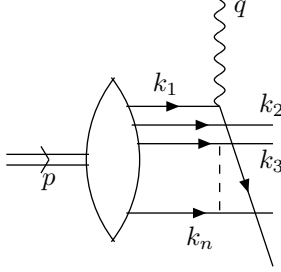


Figure 2. Parton Model for deep inelastic lepton-hadron scattering in an Infinite Momentum Frame.

an Infinite Momentum Frame (IMF) [4]. The latter is e.g. given by the following choice for the proton and vector boson momenta

$$p = (P + \frac{M^2}{2P}, \vec{0}_\perp, P), \quad q = (\frac{M\nu}{P}, \vec{q}_\perp, 0). \quad (9)$$

Writing the proton state $|p\rangle$ as a sum of multi parton states i.e. $|p\rangle = \sum_{i=1}^n |k_i\rangle$ the momenta of the latter can be expressed as

$$k_i = (x_i P + \frac{k_{i\perp}^2 + m_i^2}{2x_i P}, \vec{k}_{i\perp}, x_i P),$$

$$\text{with} \quad \sum_{i=1}^n x_i = 1. \quad (10)$$

Using the IMF representation, the life time of the multi parton state becomes

$$\tau_{part} \sim \frac{1}{\sum_{i=1}^n k_{i0} - p_0} = \frac{2P}{\sum_{i=1}^n \frac{k_{i\perp}^2 + m_i^2}{x_i} - M^2}. \quad (11)$$

If the interaction time of the vector boson with the partons is given by $\tau_{int} \sim 1/q_0 = P/M\nu$ then the scattering becomes incoherent for $\tau_{part} \gg \tau_{int}$ or

$$2M\nu + M^2 \gg \sum_{i=1}^n \frac{k_{i\perp}^2 + m_i^2}{x_i}. \quad (12)$$

The inequality above only holds if $x_i \neq 0$ or $x_i \neq 1$. From these considerations one can derive the master formula for the structure function

$$F(x, Q^2) = \sum_{a=1}^m e_a^2 f_a(x), \quad (13)$$

where x is interpreted as the fraction of the proton's momentum carried away by the parton struck by the virtual vector boson V in Fig. 1. Furthermore e_a and f_a denote the parton charge and the parton density respectively where a runs over the number of active flavours in the initial state. Notice that in QCD the relation in Eq. (13) will be modified after one has included radiative corrections. From the discussion above it is clear that at small x deep inelastic scattering becomes coherent. However the Parton Model does not give any information at which value of x this will happen. For this we have to know much more about QCD. Notice that the Infinite Momentum Frame picture is not the justification of the Parton Model. The latter can be also formulated in a Lorentz covariant way.

The real justification for the light cone expansion and the Parton Model comes from QCD. This theory gives much more firm predictions when compared with the models mentioned before and discussed hereafter. Let us enumerate some of them

- a. The Q^2 dependence of $F(x, Q^2)$.
- b. Sum rules of the type $\int_0^1 dx F(x, Q^2)$ which only depend on the flavour group and the value of the strong coupling constant α_s .
- c. Relations like the Callan-Gross relation [9] which states that the longitudinal structure function $F_L \sim 0 + O(\alpha_s)$.
- d. Factorization theorems leading to the universality of parton densities like f_a in Eq. (13). This enables us to predict distributions and cross sections of other hard processes than deep inelastic lepton-hadron scattering.
- e. Rates and distributions of jets.

Here we want to emphasize that our theoretical understanding of integrated quantities, like cross sections or the sum rules mentioned under b, is much better than what is known about differential distributions or even about the structure functions. This is all related to our ignorance about the non-perturbative properties of QCD, which means that we have to rely on models or even worse on parametrizations to describe the x -dependence of the parton densities in Eq. (13) or the fragmentation properties of quarks and gluons into hadron jets. In particular the global analysis of the parton densities requires many arbitrary free parameters. In spite of the fact that these densities allow us to describe many hard processes their arbitrariness impairs the predictive power of perturbative QCD. It is for this reason that this theory has so many competitors in particular in the small x region where diffraction plays a prominent role. Therefore better measurements of integrated quantities like the sum rules above are indispensable to show the validity of QCD although we realize that experimentally this is very hard to achieve.

2.3. Vector Meson Dominance

In the case that the process in Fig. 1 is dominated by the photon one can decompose it into a point-like and a hadron-like state i.e. $|\gamma\rangle = |\gamma_{point}\rangle + |\text{hadron}\rangle$. According to the parton model the hadronic state vanishes like $1/Q^2$. However the argument for Vector Meson Dominance (VMD) is akin to the one given for small x -physics presented below Eq. (4). If $M\nu \gg Q^2 + m^2$ where m is the mass of the hadronic state the life time of the latter in the proton's rest frame (see Fig. 3) is given by [10]

$$\tau_{had} \sim \frac{1}{p'_0 - q_0} = \frac{2\nu}{Q^2 + m^2} > 2R. \quad (14)$$

Choosing for the hadronic state the ρ -meson (lightest vector meson) one can derive, using the proton radius $R = 5 \text{ GeV}^{-1}$, the inequality $\nu > 3 + 5Q^2$ which can be considered as the characteristic value of ν for the diffractive region. The inequality above corresponds to $x < 0.1$ which belongs to the kinematic regime explored by HERA

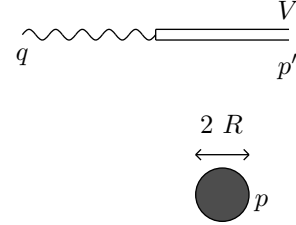


Figure 3. Photon q fluctuating into a vector meson V with momentum p' and mass m .
 $p = (M, 0)$, $q = (\nu, 0, 0, \sqrt{\nu^2 + Q^2})$,
 $p' = (\sqrt{\nu^2 + Q^2} + m^2, 0, 0, \sqrt{\nu^2 + Q^2})$.

but not quite by the old SLAC experiments. Before we discuss the predictions of VMD let us first express the structure functions into the transverse $\sigma_T(Q^2, \nu)$ and longitudinal $\sigma_L(Q^2, \nu)$ photo absorption cross sections.

$$\begin{aligned} F_2(x, Q^2) &= \frac{K}{4\pi^2\alpha} \frac{\nu Q^2}{Q^2 + \nu^2} (\sigma_T + \sigma_L), \\ F_L(x, Q^2) &= \frac{K}{4\pi^2\alpha} \frac{Q^2}{\nu} \sigma_L, \\ K &= \nu - \frac{Q^2}{2M}. \end{aligned} \quad (15)$$

In the literature there are two versions of VMD. In the older version the hadronic state was only represented by the ρ -meson [5]. Shortly after single vector meson dominance a second version was proposed called generalized VMD [11]. In the latter case one has in principle an infinite number of vector meson states which are produced in the process $e^+ + e^- \rightarrow \text{'hadrons'}$. The most general properties of VMD are

$$\begin{aligned} \sigma_T(Q^2, \nu) &= G(Q^2, \nu) \sigma_{\gamma p}(\nu), \\ \sigma_L(Q^2, \nu) &= R(Q^2, \nu) \sigma_T(Q^2, \nu). \end{aligned} \quad (16)$$

In the formulae above $\sigma_{\gamma p}$ denotes the real photon-proton ($q^2 = 0$) cross section and G is a model dependent function which can be inferred

from the process $e^+ + e^- \rightarrow \text{'hadrons'}$. The ratio R in the two models is given by

$$R \underset{Q^2 \gg m^2}{=} \xi(\nu) \frac{Q^2}{m_\rho^2} \quad \text{VMD},$$

$$R \underset{Q^2 \gg m^2}{=} \xi(\nu) \ln \left(\frac{Q^2}{m_0^2} \right) \quad \text{gen. VMD}, \quad (17)$$

where m_0 is the averaged vector meson mass. Further $\xi(\nu)$ is defined by

$$\xi(\nu) = \frac{\sigma_{tot}(V p)_{\lambda_V=0}}{\sigma_{tot}(V p)_{\lambda_V=\pm 1}}, \quad (18)$$

where $\sigma_{tot}(V p)$ denotes the total cross section for the reaction $V + p \rightarrow \text{'X'}$ and λ_V represents the helicity of the vector meson V . The main consequence of VMD is that at large Q^2 we obtain $R \gg 1$ and $F_L \sim F_2$. This is in contrast to the prediction of the quark parton model which yields $R \ll 1$ and $F_L \ll F_2$. The old SLAC data ruled out VMD with $V = \rho$ because in this case ξ is large (i.e. $\xi \sim 1.2$) and R in Eq. (17) rises linearly in Q^2 . However generalized VMD works much better since the increase of R is logarithmic and the fitted value for ξ is much less (i.e. $\xi = 0.171$) than the one found for ρ -meson dominance. We have checked that the parametrisation in [12] fits the data obtained for F_L by the H1-group [13] rather well in the region $10^{-4} < x < 5.10^{-4}$. However at larger x values i.e. for $x > 0.01$ the model in [12] breaks down because both the transverse and longitudinal cross sections become negative.

2.4. Regge Pole Model

In the Regge Pole model the structure functions are parametrised as follows

$$F_k(x, Q^2) = \sum_i \beta_{k,i}(Q^2) \left(\frac{\nu}{\nu_0} \right)^{\alpha_i(0)-1}. \quad (19)$$

Here $\alpha_i(0)$ represents the Regge trajectory at zero momentum transfer since we deal with forward Compton scattering $\gamma^* + p \rightarrow \gamma^* + p$. Further i runs over all trajectories of the particles which can be exchanged between the photon and the

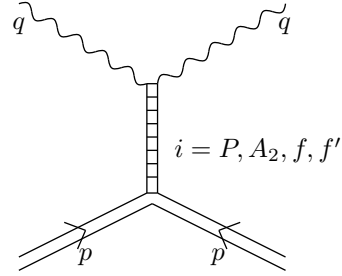


Figure 4. Regge pole exchange in forward Compton scattering.

proton among which the most prominent are the pomeron P and the mesons A_2, f, f' (see Fig. 4). Since the real photon-proton cross section behaves like $\sigma_{\gamma p}(\nu) \sim (\nu/\nu_0)^{\alpha_i(0)-1}$ a comparison between Eq. (19) and Eqs. (15), (16) reveals that VMD is a special case of the Regge Pole Model providing us with an explicit expression for $\beta_{k,i}(Q^2)$. However the Regge Pole Model does not predict scaling unless one makes the additional assumption [6]

$$\beta_{k,i}(Q^2) = b_{k,i} \left(\frac{Q_0^2}{Q^2} \right)^{\alpha_i(0)-1}, \quad (20)$$

so that one obtains

$$F_k(x) \sim \sum_i b_{k,i} x^{1-\alpha_i(0)}. \quad (21)$$

In [14] one has obtained a good fit to the data for F_2 in the range $x < 0.07$ and $0 < Q^2 < 2000 \text{ GeV}^2/c^2$ provided one allows for a Q^2 dependence of $b_{2,i}$. Moreover in addition to the soft pomeron P ($\alpha_P(0) = 1.08$) one also has to add a hard pomeron P' contribution ($\alpha_{P'}(0) \sim 1.4$). The assumption in Eq. (20) has a curious implication. This is revealed if we take the N th moment of Eq. (21) which is equal to

$$\int_0^1 dx x^{N-1} F_k(x, Q^2) = \sum_i \frac{b_{k,i}(Q^2)}{N - \alpha_i(0)}. \quad (22)$$

We will now show that this prediction is at variance with perturbative QCD. In the latter case

the N th moment is given by

$$\int_0^1 dx x^{N-1} F_k(x, Q^2) = \sum_{a=q,g} f_a^{(N)}(\mu^2) \mathcal{C}_{k,a}^{(N)} \left(\frac{Q^2}{\mu^2} \right). \quad (23)$$

Here μ represents the factorization as well as the renormalization scale. Since in the Regge Pole Model $\alpha_i(0)$ is independent of Q^2 the location of the singularities in the N -plane (see Eq. (22)) does not depend on Q^2 . In the scaling parton model where $\mathcal{C}^{(N)} = 1$ the Regge pole behaviour is also exhibited by the parton densities $f_a^{(N)}$. However in perturbative QCD new poles will appear in the N -plane because of the behaviour

$$\mathcal{C}_{k,a}^{(N)} \sim \left(\frac{\alpha_s(\mu^2)}{\pi} \right)^m \gamma_{ab}^{(N)} \ln \frac{Q^2}{\mu^2}. \quad (24)$$

The anomalous dimensions $\gamma_{ab}^{(N)}$ contain poles in the N -plane different from those given by the Regge Pole Model. For example we have

$$\gamma_{ab}^{(N)} \sim \frac{1}{N-1}, \frac{1}{N}, \frac{1}{N+1} \quad \text{etc.} \quad (25)$$

From Eq. (24) we infer that the appearance of the pole terms on the right hand side of Eq. (23) depends on the value of Q^2 which is in contradiction with the assumption in the Regge Pole Model. Notice that the singularities at $N = 1$ disappear if the pole terms of the type $1/(N-1)^l$ are re-summed in all orders of perturbation theory using the BFKL equation [7]. This follows from the BFKL characteristic function

$$\chi(a_s \gamma_{gg}(N)) = \frac{N-1}{6a_s}, \quad a_s = \frac{\alpha_s}{\pi}, \quad (26)$$

which does not contain a singularity in $\gamma_{gg}(N)$ at $N = 1$. Unfortunately such an equation is not known for the other poles given by $N \geq 0$. However in principle there is no contradiction between perturbative QCD and the Regge Pole Model provided one drops the assumption made in Eq. (20) leading to Eq. (21). Therefore the Regge poles show up in the angular momentum plane but not in the N -plane (moment-plane). Notice that N is the quantum number associated with the angular momentum in the four dimensional Euclidean

plane. Hence we conclude that the assumption made in Eq. (20) (see [6]) only works in the case of the old scaling parton model but not for QCD. Hence we disagree with the conclusions of [14] that Regge poles contradict the singularity structure in the N -plane predicted by perturbative QCD. Moreover we want to emphasize that the singularities at $N = 1$ in $\gamma_{ab}^{(N)}$ (25), which are called the leading poles, pose no harm for the convergence of the perturbation series. First, as has been shown in a model [15], the residues of the sub-leading singularities at $N = 0, -1, -2, \dots$ are much larger than the one corresponding to the leading pole. Therefore the latter does not dominate the asymptotic behaviour of the coefficient function for $z \rightarrow 0$. The second reason can be traced back to the structure function, appearing in Eq. (23), which can be written as a convolution of parton densities and coefficient functions in Bjorken x -space. Since these densities $f_a(x/z)$ vanish in the region $z \sim x$ the effect of the leading poles in the coefficient function, which behave in z -space like $(\ln^m z)/z$, will be considerably reduced. A systematic study regarding the phenomenological meaning of these so called leading poles or small x -terms is presented in [16].

3. Issues in QCD which are relevant for large x and Q^2

3.1. NNLO analysis of the structure functions

If one would like to have a test of perturbative QCD which can be performed on the same level of accuracy as achieved in $e^+ e^-$ physics it is necessary to get a next-to-next-to-leading order (NNLO) description of the structure functions. Notice that some quantities like $R(e^+ e^- \rightarrow 'X')$ or $\Gamma(Z \rightarrow \text{hadrons})$ are already known up to order α_s^3 so that they are even one order higher in accuracy than the NNLO expression of $F_k(x, Q^2)$. The latter can be used to check the QCD prediction for its evolution with respect to Q^2 and to extract the value of α_s which can be compared with the results obtained from the LEP and SLC experiments. The ingredients for the NNLO anal-

ysis are the order α_s^2 corrected coefficients [17] and the order α_s^3 corrected anomalous dimensions (splitting functions). However the three-loop contributions to the anomalous dimensions $\gamma_{ab}^{(N)}$ are only known for $N \leq 10$ [18] except for the leading n_f part, where n_f denotes the number of flavours, which is computed in [19]. For the computation of the integrals corresponding to the three-loop graphs one has to make a thorough study of the transcendental functions which show up in the splitting functions $P_{ab}(z)$ and the anomalous dimensions $\gamma_{ab}^{(N)}$. Typical functions which appear in $P_{ab}(z)$ are the Nielsen integrals corresponding to finite and infinite harmonic sums in $\gamma_{ab}^{(N)}$. A study of Nielsen integrals and harmonic sums is made in [20] and [21]. The computation of $\gamma_{ab}^{(N)}$ for general N is very tedious and its feasibility is still under study. Therefore one should try to make an estimate of the three-loop anomalous dimensions. For this estimate one can use all the information on super-symmetric and conformal relations available in the literature [26]. One also knows the leading and sub-leading pole terms of the type $\gamma_{ab}^{(N)} \sim 1/(N-1)^m$ from the solution of the BFKL characteristic function [7] which is known up to NLO. One also gets some input from the behaviour at large N which is conjectured for the $\overline{\text{MS}}$ -scheme in [22]. According to the last reference the anomalous dimension behaves like $\gamma_{ab}^{(N)} \sim \ln N$ in all orders of α_s for $N \rightarrow \infty$. Another interesting question is whether in the $\overline{\text{MS}}$ -scheme the NNLO corrected structure functions are dominated by the coefficient functions rather than the anomalous dimensions so that the latter play a subordinate role. Using some of the ideas above one has already made a NNLO analysis of the structure function $F_3(x, Q^2)$ in [23]. One of the interesting results is that higher twist ($\tau = 4$, see Eq. (6)) contributions get smaller when NNLO corrections are included. Recently a similar analysis was performed for the singlet and non-singlet part of the structure function $F_2(x, Q^2)$ in electro-production in [24].

3.2. Measurement of α_s

It is expected that NNLO corrections to the structure functions diminish the theoretical error

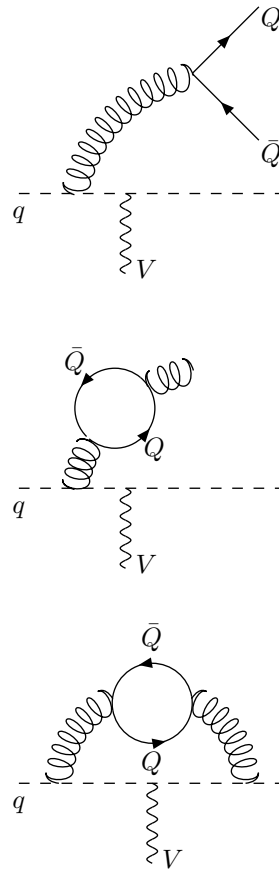


Figure 5. Heavy flavour production $V + q \rightarrow q + Q + \bar{Q}$ including virtual corrections ($V = \gamma, W, Z$).

on α_s by about 50 % with respect to NLO. There is also a strong dependence on the cut Q_{cut}^2 imposed on the data set [25]. A larger cut leads to a decrease of $\alpha_s(M_Z^2)$ by about 0.002. Another issue is the treatment of heavy flavour contributions to the coupling constant. Usually this is done by imposing the following matching conditions

$$\alpha_s(n_f, \Lambda_{n_f}, a m^2) = \alpha_s(n_f + 1, \Lambda_{n_f+1}, a m^2), \quad (27)$$

where m is the mass of the heavy flavour. In the literature one takes $a = 1$ which means that for $Q^2 > m^2$ the heavy flavour behaves as a massless quark. However this does not follow from perturbation theory. An example is shown in [27]. The heavy flavour contribution to the structure function appears for the first time in order α_s^2 (see Fig. 5) provided we assume that the initial hadron state does not contain a heavy quark. The easiest way to study these contributions is to look at sum rules e.g. the Gross-Llewellyn Smith sum rule [28] which up to order α_s^2 is given by

$$\begin{aligned} \int_0^1 dx \left[F_3^{\bar{\nu}p}(x, Q^2) + F_3^{\nu p}(x, Q^2) \right] = \\ 6 \left[1 + \frac{\alpha_s(n_f, Q^2)}{\pi} a_1 + \left(\frac{\alpha_s(n_f, Q^2)}{\pi} \right)^2 \{ a_2 \right. \\ \left. + H \left(\frac{Q^2}{m^2} \right) \} \right]. \end{aligned} \quad (28)$$

Here a_1, a_2 represent the light quark and gluon contributions [17], [29]. The heavy quark contribution denoted by H [27] behaves asymptotically as

$$\begin{aligned} H \left(\frac{Q^2}{m^2} \right) &\xrightarrow{m^2 \gg Q^2} \frac{Q^2}{m^2}, \\ H \left(\frac{Q^2}{m^2} \right) &\xrightarrow{Q^2 \gg m^2} \frac{1}{6} a_1 \ln \frac{Q^2}{m^2} + b_2. \end{aligned} \quad (29)$$

The asymptotic behaviour for $m^2 \gg Q^2$ follows from the decoupling theorem so that at small scales the heavy quark does not contribute to the sum rule. The asymptotic behaviour for $Q^2 \gg m^2$ can be interpreted that the heavy flavour behaves like a light quark which is revealed by the mass singular logarithm. One can

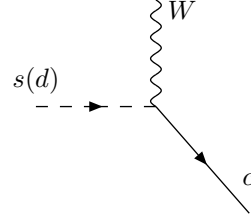


Figure 6. Charm production $W + s(d) \rightarrow c$.

check that the exact expression becomes equal to the asymptotic one for $Q^2 > 40 m^2$ which implies that a in Eq. (27) should be chosen to be 40 instead of 1. Only for this value it makes sense to re-sum the large logarithm on the right-hand side in Eq. (29). This is achieved by absorbing the logarithm $\ln(Q^2/m^2)$ into the running coupling constant

$$\alpha_s(n_f + 1, Q^2) = \frac{\alpha_s(n_f, Q^2)}{1 - \frac{\alpha_s(n_f, Q^2)}{6\pi} \ln \frac{Q^2}{m^2}}. \quad (30)$$

After having removed the function H on the right-hand side of Eq. (28), $\alpha_s(n_f, Q^2)$ has to be replaced by $\alpha_s(n_f + 1, Q^2)$ so that the perturbation series for the sum rule is represented in an $n_f + 1$ flavour scheme. The lesson which one can draw from this calculation is that it is not the virtuality p^2 of the gluon, which is coupled to the heavy quark anti-quark pair in Fig. 5, but the value of the external kinematic scale Q^2 which is relevant for the heavy flavour threshold in the running coupling constant and the value of a in Eq. (27). Of course it might happen that p^2 represents a physical observable like the momentum transfer in e.g. quark-quark scattering. Here it turns out that if $-p^2 \geq m^2$ the flavour has to be treated as a light quark.

3.3. Down and strange quark densities at large x

One of the goals of future HERA experiments is to provide us with a better determination of the down $d(x)$ and strange $s(x)$ quark densities. To

start with the former the ratio $d(x)/u(x)$ can be extracted from the cross sections of the charged current interactions from the ratio

$$\frac{\sigma_{CC}(e^+ p)}{\sigma_{CC}(e^- p)}. \quad (31)$$

It is not excluded that one can expect $d(x)/u(x) \rightarrow \text{const.}$ when $x \rightarrow 1$ which is in contrast with present parametrisations. Notice that until now information on $d(x)$ is available from the following observables.

- a. The first quantity is given by

$$\frac{F_2^{\mu n}(x, Q^2)}{F_2^{\mu p}(x, Q^2)}. \quad (32)$$

Until now the structure functions above are extracted from fixed target experiments so that one has to correct for nuclear binding effects [30]. This means that $d(x)$ might deviate from the parametrisations existing in the literature.

- b. Another observable is the lepton asymmetry in W -production in proton anti-proton colliders given by the reaction

$$\begin{aligned} p + \bar{p} &\rightarrow W^+ (W^-) + 'X' \\ &\quad | \\ &\rightarrow l^+ \nu_l (l^- \bar{\nu}_l). \end{aligned} \quad (33)$$

The strange quark density can be measured in charm quark production in the charged current process $e^-(e^+) + p \rightarrow \nu_e(\bar{\nu}_e) + 'X'$. The basic reactions are given by (Fig. 6)

$$s + W^+ \rightarrow c, \quad \bar{s} + W^- \rightarrow \bar{c}. \quad (34)$$

It is found that the radiative corrections to the processes above are very small. The latter are represented by the one-loop corrections to reactions (34) and the gluon bremsstrahlung (Fig. 7)

$$s + W^+ \rightarrow c + g, \quad \bar{s} + W^- \rightarrow \bar{c} + g. \quad (35)$$

However the determination of the strange quark density is hampered by the following backgrounds. The first one is given by the process

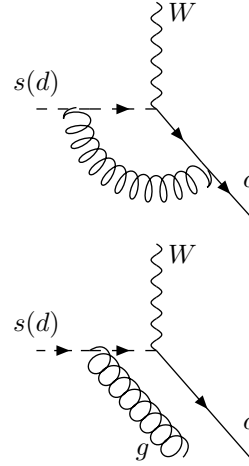


Figure 7. Charm production $W + s(d) \rightarrow c + g$ including radiative corrections.

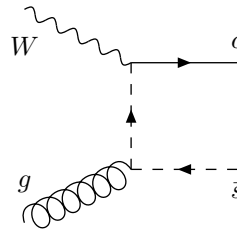


Figure 8. Charm production in $W + g \rightarrow c + \bar{s}$ (gluon-boson fusion).

$$d + W^+ \rightarrow c. \quad (36)$$

Although this process is Cabibbo suppressed it is enhanced when it appears in $e^+ + p \rightarrow \bar{\nu}_e + 'X'$ because in this case the d becomes a valence quark and $d_v(x) \gg s(x)$. Another background is the gluon-boson fusion reaction (Fig. 8)

$$g + W^+ \rightarrow c + \bar{s}, \quad g + W^- \rightarrow \bar{c} + s, \quad (37)$$

which dominates the cross section $d\sigma/dx$ for $x < 0.1$. Higher order corrections to the reaction above [31] are quite appreciable in particular for $F_3(x, Q^2)$ but less for $F_2(x, Q^2)$. Therefore one can only determine $s(x)$ when the gluon density is accurately known in the region $5 \cdot 10^{-3} < x < 0.1$. To circumvent this problem the authors in [32] have proposed to measure the D -mesons which emerge from the (anti)charm quarks. Instead of $d\sigma/dx$ one has to compute

$$\frac{d^2\sigma}{dx dz} \sim \sum_a f_a \otimes H_a^c \otimes D_c, \quad (38)$$

where H_a^c ($a = q, g$) denote the heavy quark coefficient functions corresponding to reactions (34), (35) and (37). The function $D_c(z)$ describes the fragmentation of the c -quark into the D -meson with $p_D = z p_c$. It appears that for $z < 0.2$ the gluon-boson fusion dominates charm quark production so that one has to impose a cut on z in order to suppress this background. In this case one obtains the quantity

$$\frac{d\sigma}{dx} = \int_{0.2}^1 dz \frac{d^2\sigma}{dx dz}, \quad (39)$$

leading to the result $d\sigma^{NLO} \sim d\sigma^{LO}$ so that the Born reaction in Eq. (34) becomes dominant and the extraction of the strange quark density is possible.

3.4. Factorization and renormalization scale dependence

As one knows physical quantities like structure functions and cross sections are scheme independent which implies that they do not depend on the choice made for the factorization scale μ_F and the renormalization scale μ_R . However finite order perturbation theory violates this property as

one can see as follows. Take as an example the N th moment of a structure function given by

$$F^{(N)}(Q^2) = f_q^{(N)}\left(\frac{Q_0^2}{\mu^2}, a_s(\mu^2)\right) C_q^{(N)}\left(\frac{Q^2}{\mu^2}, a_s(\mu^2)\right), \quad (40)$$

with the quark density (for the definition of a_s see Eq. (26))

$$f_q^{(N)} = \left[1 + a_s(\mu^2)(A_q^{(1)} - c_q^{(1)})\right] \times \left[\frac{a_s(\mu^2)}{a_s(Q_0^2)}\right]^{\gamma_{qq}^{(0)}/2\beta_0} f_q^{(N)}(Q_0^2). \quad (41)$$

and the coefficient function

$$C_q^{(N)} = \left[1 + a_s(Q^2)A_q^{(1)} + a_s(\mu^2)(c_q^{(1)} - A_q^{(1)})\right] \left[\frac{a_s(Q^2)}{a_s(\mu^2)}\right]^{\gamma_{qq}^{(0)}/2\beta_0}, \quad (42)$$

Notice that we have chosen $\mu_F = \mu_R = \mu$ for simplicity. Further $A_q^{(1)}$ is a scheme independent combination of the the anomalous dimensions and the coefficient $c_q^{(1)}$. The latter is the order α_s contribution to the series expansion of the coefficient function $C_q^{(N)}$ and is scheme dependent. The lowest order terms in the perturbation series for the anomalous dimension and the beta-function are given by $\gamma_{qq}^{(0)}$ and β_0 respectively. When we multiply the coefficient function by the quark density all scheme dependence cancels up to order a_s . However the order a_s^2 term depends on the scheme and the scale μ because of the missing two-loop coefficient function and the three-loop anomalous dimension. If one varies the scale like what is usually done by $Q/2 < \mu < 2Q$ then the variation in $F^{(N)}$ is wholly due to the spurious order a_s^2 term. Therefore one can raise the question whether this scale variation is a good estimate of the theoretical error due to the absence of higher order QCD corrections. Moreover the scale variation performed on NLO quantities only probes the effect of the Born process on the NLO corrected cross section. The latter has the typical form

$$\hat{\sigma}_{ab}^{(1)} = \bar{\sigma}_{ab}^{(1)} + \frac{1}{2} P_{cb}^{(0)} \otimes \hat{\sigma}_{ac}^{(0)} \ln\left(\frac{Q^2}{\mu_F^2}\right)$$

$$-\beta_0 \hat{\sigma}_{ab}^{(0)} \ln \left(\frac{Q^2}{\mu_R^2} \right). \quad (43)$$

Here $\hat{\sigma}_{ab}^{(0)}$ and $\hat{\sigma}_{ab}^{(1)}$ represent the lowest (Born) and the first order cross section respectively. The lowest order splitting function is denoted by $P_{cb}^{(0)}$. The quantity $\bar{\sigma}_{ab}^{(1)}$ contains all first order contributions originating from new production mechanism's. From Eq. (43) one infers that all scale dependent logarithms are multiplied by the Born cross section only. In the case that $\bar{\sigma}_{ab}^{(1)}$ is large the latter gives a better indication about the theoretical error due to higher order corrections than a simple scale variation of the NLO hadronic cross section.

4. Re-summation of large corrections occurring at small and large x

From the computations of splitting functions $P_{ab}(x)$ and coefficient functions $C_{k,a}(x, Q^2/\mu^2)$ we infer that large corrections can appear at

- a. $x \rightarrow 0$ (soft gluon exchanges)
- b. $x \rightarrow 1$ (soft gluon bremsstrahlung)

However the relevance of these corrections does not only depend on the quantities above but also on the behaviour of the parton densities. This one can see by a study of the structure functions given by

$$F_k(x, Q^2) \sim \sum_a \int_x^1 \frac{dz}{z} f_a\left(\frac{x}{z}, \mu^2\right) C_{k,a}\left(z, \frac{Q^2}{\mu^2}\right). \quad (44)$$

Because of the convolution integral it might happen that $f_a(x/z, \mu^2)$ vanishes in the regions $z \rightarrow 0$ or $z \rightarrow 1$ so that the total contribution to the structure functions is small in spite of the fact that the coefficient functions and the splitting functions blow up in these regions. Therefore a re-summation of these non-dominant corrections will lead to an overestimate of their effect on the physical quantities.

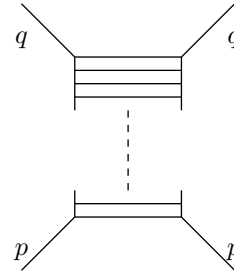


Figure 9. Ladder graph in Φ_6^3 -theory.

4.1. Large corrections at small x

The large corrections occurring for $z \rightarrow 0$ are due to soft gluon exchanges in the t -channel. They have the following form

$$\begin{aligned} C_{k,a}^{(l)}(z, 1) &\sim \frac{\ln^{l-2} z}{z} \quad l \geq 2, \\ P_{ab}^{(l)}(z) &\sim \frac{\ln^l z}{z} \quad l \geq 0. \end{aligned} \quad (45)$$

Because the singular behaviour is due to gluon exchange it only appears in the singlet part of the coefficient functions and splitting functions. The re-summation of these logarithms is performed by the BFKL equation [7]. However one has to be careful with the interpretation of the solution of this equation which will be defined as $\mathcal{C}^{BFKL}(z)$. One cannot claim that the latter represents the asymptotic form of the exact coefficient function $\mathcal{C}^{EXACT}(z)$ in the limit $z \rightarrow 0$. This can be shown in Φ_6^3 -theory where the exact solution [33] is known for the ladder diagrams (see Fig. 9). In this case one can also re-sum the leading terms given at each order [15] which can be considered as the analogue of the BFKL-solution but now in the case of Φ_6^3 -theory. However this re-summation leads to an answer which differs by a factor of two and larger from the exact result taken in the limit $z \rightarrow 0$. This means that also non-leading terms determine the asymptotic expression for the ladder graphs. Since the non-leading order terms also appear in non-planar di-

agrams, which do not belong to the class of ladder graphs, one cannot even claim that the asymptotic expression for the total coefficient function is determined by the ladder approximation only. Since the exact expression for the re-summation of a subset of graphs, analogous to the ladder approximation, is unknown in QCD it is very hard to judge what the relation is between the BFKL solution and the perturbative QCD result in the small x -region.

4.2. Large corrections at large x

The large corrections which appear in the limit $z \rightarrow 1$ are due to soft gluon radiation. They have the following form when the l th order quantities are presented in the $\overline{\text{MS}}$ -scheme for $\mu^2 = Q^2$

$$\begin{aligned} \mathcal{C}_{k,a}^{(l)}(z, 1) &\sim \left(\frac{\ln^{2l-1}(1-z)}{1-z} \right)_+ \quad l \geq 1, \\ P_{ab}^{(l)}(z) &\sim \left(\frac{1}{1-z} \right)_+ \quad l \geq 0. \end{aligned} \quad (46)$$

Notice that the expression for the splitting function is a conjecture made in [22]. The singularity structure given in the equation above is typical for the non-singlet coefficient function contributing to F_2 and F_3 . If the coefficient function in the above equation is convoluted with regular functions the singularity structure becomes much milder. In this case they have the form

$$\mathcal{C}_{k,a}^{(l)}(z, 1) \sim a_l \ln^{2l-2}(1-z) \quad l \geq 2. \quad (47)$$

Examples of this behaviour can be found for the coefficient functions contributing to the longitudinal structure function F_L and the cross section for direct photon production. The study of the logarithms which appear in the coefficient function of Eq. (47) has a twofold purpose.

- Prediction of the coefficients a_l in Eq. (47) and a comparison with the results obtained from the exact expression. In this way one can check the exact calculation.
- The investigation of the coefficients a_l will reveal how one has to re-sum the large logarithms.

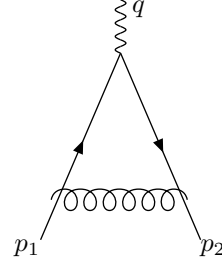


Figure 10. One-loop vertex graph contributing to $F^{(1)}(Q^2)$.

First we would like to discuss the work done in [34] to re-sum the logarithmic terms occurring in the longitudinal coefficient function contributing to F_L . Up to $l = 2$ one obtains the following form when the scales are chosen to be $\mu_F = \mu_R = Q$

$$\begin{aligned} \mathcal{C}_{L,q}^{(0)}(z, 1) &= 0, \quad \mathcal{C}_{L,q}^{(1)}(z, 1) = C_F z, \\ \mathcal{C}_{L,q}^{(2)}(z, 1) &= C_F^2 \left[\frac{1}{2} \ln^2(1-z) + \left(\frac{9}{4} - 2\zeta(2) \right) \right. \\ &\quad \times \ln(1-z) \left. \right] + C_A C_F \left[(\zeta(2) - 1) \ln(1-z) \right] \\ &\quad - \frac{1}{4} \beta_0 C_F \ln(1-z) + \text{regular terms in } z, \end{aligned} \quad (48)$$

Here C_F and C_A represent the well-known colour factors. The re-summation of these logarithms is easier when one performs the Mellin transformation. In the limit $N \rightarrow \infty$ one obtains

$$\begin{aligned} \mathcal{C}_{L,q}^{(N),(2)}(z, 1) &= \frac{C_F}{2N} \left[\gamma_K^{(0)} \ln^2 \frac{N}{N_0} \right. \\ &\quad \left. - (\gamma_{J'}^{(1)} - \frac{1}{2} \beta_0) \ln \frac{N}{N_0} \right], \end{aligned} \quad (49)$$

and $\gamma_{J'}$ is the anomalous dimension of a certain operator determining the jet function [34]. The quantity γ_K represents the Sudakov anomalous dimension and it is related to the infrared structure of a gauge theory like QCD. It also occurs in the vertex correction to the quark-gluon vertex represented by $F(Q^2)$. Using n -dimensional regularization with $\varepsilon = n - 4$ and $p_1^2 = p_2^2 = 0$ one

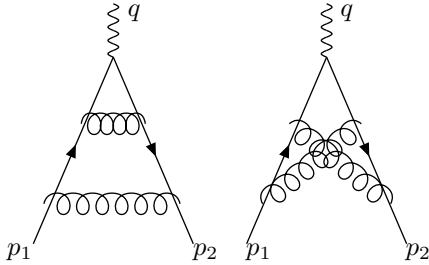


Figure 11. Some two-loop vertex graphs contributing to $F^{(2)}(Q^2)$.

obtains for the one-loop correction (see Fig. 10)

$$F^{(1)}(Q^2) = \left(\frac{Q^2}{\mu^2}\right)^{\varepsilon/2} \left[\frac{\gamma_K^{(0)}}{\varepsilon^2} + \dots \right]. \quad (50)$$

The two-loop expression (Fig. 11) looks like

$$F^{(2)}(Q^2) = \left(\frac{Q^2}{\mu^2}\right)^{\varepsilon} \left[\frac{(\gamma_K^{(0)})^2}{2\varepsilon^4} + \left(\frac{1}{\varepsilon^3}\right) \frac{\gamma_K^{(1)} + \dots}{2\varepsilon^2} + \dots \right]. \quad (51)$$

From the coefficients of the leading pole terms one infers that the re-summed Sudakov vertex correction gets an exponential form [35], [36]. Because of the analogy between the $\ln N$ terms in the coefficient function and the $1/\varepsilon$ poles in $F(Q^2)$ we expect that the same will happen in the former case. The re-summed expression for Eq. (49) has been found in [34].

A similar attempt to re-sum the large logarithmic terms has been made for the partonic cross sections (coefficient functions) which appear in direct photon production given by

$$H_1(p_1) + H_2(p_2) \rightarrow \gamma(E_T) + X', \quad (52)$$

$$S = (p_1 + p_2)^2, \quad x = \frac{2 E_T}{\sqrt{S}}.$$

In the reaction above H_1 and H_2 denote the incoming hadrons and E_T is the transverse energy of the photon. For this process the l th order finite

partonic cross section has the form

$$\hat{\sigma}_{ab}^{(l)}(z) \sim \hat{\sigma}_{ab}^{(0)}(z) \left[d_{l,2l} \ln^{2l}(1-z) + d_{l,2l-1} \ln^{2l-1}(1-z) + \dots \right] \quad l \geq 1, \quad (53)$$

where $\sigma_{ab}^{(0)}$ denote the Born cross sections corresponding to the processes in Fig. 12. Notice that $\sigma_{qg}^{(0)}$ is dominant in $p-N$ scattering whereas $\sigma_{q\bar{q}}^{(0)}$ becomes more important in $p-\bar{p}$ collisions. Like in the case of the longitudinal coefficient function it is more convenient to take the Mellin transform of the partonic cross sections which become

$$\hat{\sigma}_{ab}^{(N),(l)} \sim \hat{\sigma}_{ab}^{(N),(0)} \left[c_{l,2l} \ln^{2l} \frac{N}{N_0} + c_{l,2l-1} \ln^{2l-1} \frac{N}{N_0} + \dots \right], \quad l \geq 1. \quad (54)$$

The re-summation of the $\ln N$ terms is carried out in [37] (see also [38], [39]) and leads to exponentiation analogous to what we have discussed above. The goal of this re-summation was to get a better description of the transverse energy E_T distribution of the direct photon. It turns out [37] that the re-summation leads to an improvement of the factorization scale dependence with respect to the exact NLO hadronic cross section. However the discrepancy between $d\sigma^{NLO}/dE_T$ and the data, in particular those coming from the E706 experiment, remains. This occurs in the region $x < 0.57$ where $E_T < 9$ GeV and $\sqrt{S} = 31.6$ GeV. There is also a little discrepancy for the UA6 experiment in the region $x < 0.5$ where $E_T < 6$ GeV and $\sqrt{S} = 24.3$ GeV. Notice that these regions lie outside the large x -region which is close to 1 where soft gluons dominate. Therefore one cannot expect that soft gluon re-summation will cure the discrepancy found at smaller x . Several proposals have been made to describe the data at smaller transverse energy. One is made in [40] where it is assumed that the initial state partons have an intrinsic transverse momentum. Another point of view is presented in [41] claiming that the low E_T data are inconsistent among the various experiments.

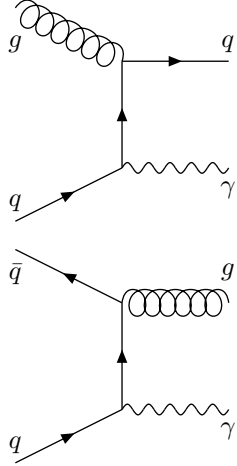


Figure 12. The Born contributions to direct photon production $q + g \rightarrow q + \gamma$, $q + \bar{q} \rightarrow g + \gamma$.

5. Conclusions

Summarizing this talk we conclude

1. Since HERA started to explore the small x -region one has seen a resurgence of models which were ruled out by fixed target deep inelastic experiments carried out at large x i.e. $0.01 < x < 1$. Some of them are discussed like for instance the Regge Pole Model and Vector Meson Dominance. The BFKL approach which became popular with the advent of HERA data merges ideas taken from the Regge Pole Model as well as from QCD. None of these models is able to predict the Q^2 -evolution of the deep inelastic structure functions contrary to QCD where the evolution follows from the renormalization group equations. However until now the x -dependence of the structure function cannot be predicted by QCD. Therefore as far as the small x -behaviour is concerned the aforementioned models cannot be ruled out since they give an equally good description of the data.

2. Future experiments at HERA and fixed target experiments at FNAL will explore the large x -region ($x > 0.01$) where there is no alternative model to perturbative QCD.
3. The future deep inelastic lepton-hadron experiments have to lead to precision tests of QCD akin to the program carried out for $e^+ e^-$ colliders like LEP and SLC. In particular one has to perform,
 - a. An accurate determination of the strong coupling constant α_s which can be obtained from structure functions as well as jet distributions.
 - b. A study of heavy flavour thresholds in α_s and the structure functions $F_k(x, Q^2)$.
 - c. A better estimate of large corrections in the perturbation series for physical quantities.
 - d. The computation of the three-loop splitting functions (anomalous dimensions) in order to give a full NNLO analysis of $F_k(x, Q^2)$.

REFERENCES

1. E.D. Bloom et al., Phys. Rev. Lett. **23** (1969) 930;
M. Breidenbach et al., Phys. Rev. Lett. **23** (1969) 935.
2. W. Bartel et al., Phys. Lett. **B28** (1968) 148;
W. Albrecht et al., DESY Report 69/7 (1969).
3. R.A. Brandt, G. Preparata, Nucl. Phys. **B27** (1971) 541;
Y. Frishman, Ann. Phys. (NY) **66** (1971) 373.
4. R.P. Feynman, Phys. Rev. Lett. **23** (1969) 1415;
S.D. Drell, T.M. Yan, Ann. Phys. (NY) **66** (1971) 578.
5. J.J. Sakurai, Phys. Rev. Lett. **22** (1969) 981;
C.F. Cho and J.J. Sakurai, Phys. Lett. **B31** (1970) 22.
6. H. Harari, Phys. Rev. Lett. **22** (1969) 1078;
H.D.I. Abarbanel, M.I. Goldberger, S.B. Treiman, Phys. Rev. Lett. **22** (1969) 500.

7. E.A. Kuraev, L.N. Lipatov, V.S. Fadin, Sov. Phys. JETP **45** (1977) 199;
Y. Balitskii, L.N. Lipatov, Sov. J. Nucl. Phys. **28** (1978) 822.
8. V.N. Gribov, B.L. Ioffe, I.Ya. Pomeranchuk, Sov. J. Nucl. Phys. **2** (1966) 549;
B.L. Ioffe, Phys. Lett. **B30** (1969) 123.
9. C.G. Callan, D.J. Gross, Phys. Rev. Lett. **22** (1969) 156.
10. H.T. Nieh, Phys. Rev. D1 (1970) 3161, *ibid.* **D7** (1973) 4301.
11. J.J. Sakurai, D. Schildknecht, Phys. Lett. **B40** (1972) 121; B. Gorczyca, D. Schildknecht, Phys. Lett. **B47** (1973) 71.
12. D. Schildknecht, H. Spiesberger, hep-ph/9707447.
13. C. Adloff et al. (H1-collaboration), Phys. Lett. **B393** (1997) 452.
14. J.H. Cudell, A. Donachie, P.V. Landshoff, Phys. Lett. **B448** (1999) 281; P.V. Landshoff, these proceedings, hep-ph/9905230.
15. J. Blümlein, W.L. van Neerven, Phys. Lett. **B450** (1999) 412.
16. J. Blümlein, A. Vogt, Phys. Rev. **D57** (1998) R1, Phys. Rev. **D58** (1998) 014020.
17. E.B. Zijlstra, W.L. van Neerven, Phys. Lett. B272 (1991) 127, Phys. Lett. **B273** (1991) 476, Phys. Lett. B297 (1992) 377, Nucl. Phys. **B383** (1992) 525.
18. S.A. Larin, T. van Ritbergen and J.A.M. Vermaseren, Nucl. Phys. **B427** (1994) 41;
S.A. Larin et al., Nucl. Phys. **B492** (1997) 338.
19. J.A. Gracey, Phys. Lett **B322** (1994) 141;
J.A. Benett and J.A. Gracey, Phys. Lett. **B432** (1998) 209, Nucl. Phys. **B517** (1998) 241.
20. J. Blumlein, S. Kurth, hep-ph/9708388, hep-ph/9810241, Phys. Rev. **D** in print.
21. E. Remiddi, J.A.M. Vermaseren, hep-ph/9905237.
22. A. Gonzalez-Arroyo, C. Lopez, F.J. Yndurain, Nucl. Phys. **B153** (1979) 161.
23. A.L. Kataev, G. Parente and A.V. Sidorov, hep-ph/9809500, hep-ph/9904332.
24. J. Santiago, F.J. Yndurain, hep-ph/9904344.
25. A. Vogt, these proceedings.
26. A.P. Bukhvostov et al., Nucl. Phys. **B258** (1985) 601.
27. J. Blümlein, W.L. van Neerven, Phys. Lett. **B450** (1999) 417.
28. D.J. Gross, C.H. Llewellyn Smith, Nucl. Phys. **B14**(1969) 337.
29. S.G. Gorishni, S.A. Larin, Nucl. Phys. **B283** (1987) 452.
30. A. Bodek, U.K. Yang, hep-ph/9809480.
31. M. Buza, W.L. van Neerven, Nucl. Phys. **B500** (1997) 301.
32. S. Kretzer and M. Stratmann, hep-ph/9902426.
33. C. Lovelace, Phys. Lett. **B55** (1975) 187; Nucl. Phys. **B95** (1975) 12.
34. R. Akhoury, G. Sotiropoulos, G. Sterman, hep-ph/9903442.
35. A. Sen, Phys. Rev. **D27** (1983) 2997.
36. J. C. Collins in "Perturbative Quantum Chromodynamics", Ed. A.H. Mueller, pg.573.
37. S. Catani et al., hep-ph/9903436
38. E. Laenen, G. Oderda, G. Sterman, Phys. Lett. **B438** (1998) 173.
39. N. Kidonakis, hep-ph/9902484.
40. A.D. Martin et al., Eur. Phys. J. **C4** (1998) 463.
41. P. Aurenche et al., hep-ph/9811382.